Chemistry Central Journal

Open Access

Selective Iron(III) ion uptake using CuO-TiO$_2$ nanostructure by inductively coupled plasma-optical emission spectrometry

Mohammed M Rahman[1,2*], Sher Bahadar Khan[1,2], Hadi M Marwani[1,2], Abdullah M Asiri[1,2] and Khalid A Alamry[2]

Abstract

Background: CuO-TiO$_2$ nanosheets (NSs), a kind of nanomaterials is one of the most attracting class of transition doped semiconductor materials due to its interesting and important optical, electrical, and structural properties and has many technical applications, such as in metal ions detection, photocatalysis, Chemi-sensors, bio-sensors, solar cells and so on. In this paper the synthesis of CuO-TiO$_2$ nanosheets by the wet-chemically technique is reported.

Methods: CuO-TiO$_2$ NSs were prepared by a wet-chemical process using reducing agents in alkaline medium and characterized by UV/vis., FT-IR spectroscopy, X-ray photoelectron spectroscopy (XPS), powder X-ray diffraction (XRD), and field-emission scanning electron microscopy (FE-SEM) etc.

Results: The structural and optical evaluation of synthesized NSs were measured by XRD pattern, Fourier transform infrared (FT-IR) and UV–vis spectroscopy, respectively which confirmed that the obtained NSs are well-crystalline CuO-TiO$_2$ and possessing good optical properties. The morphological analysis of CuO-TiO$_2$ NSs was executed by FE-SEM, which confirmed that the doped products were sheet-shaped and growth in large quantity. Here, the analytical efficiency of the NSs was applied for a selective adsorption of iron(III) ion prior to detection by inductively coupled plasma-optical emission spectrometry (ICP-OES). The selectivity of NSs towards various metal ions, including Au(III), Cd(II), Co(II), Cr(III), Fe(III), Pd(II), and Zn(II) was analyzed.

Conclusions: Based on the selectivity study, it was confirmed that the selectivity of doped NSs phase was the most towards Fe(III) ion. The static adsorption capacity for Fe(III) was calculated to be 110.06 mgg^{-1}. Results from adsorption isotherm also verified that the adsorption process was mainly monolayer-adsorption onto a surface containing a finite number of CuO-TiO$_2$ NSs adsorption sites.

Keywords: CuO-TiO$_2$ nanosheets, Wet-chemical process, Optical property, Structural property, Adsorption isotherm, Iron(III) ion detection

Introduction

Transition-metal doped semiconductor nanomaterial have attracted significant attention due to their potential applications in fabrication of nano-scale electronics, electro-analytical, selective metal-ions detection, opto-electronics, biological devices, electron field-emission sources for emission displays, bio-chemical detections, surface-enhanced Raman properties, and immense-potential applications etc. [1,2]. It is exhibited a regular morphological nanostruc

ture, which composed a number of regular phases with geometrically-coordinated metals and oxide atoms along the axes. Doped materials have also concerned significant research effort for their exceptional and outstanding properties as well as versatile applications [3,4]. In last decade, nano-sized transition-metal oxides have been widely studied as promising anodes for Laser-Induced Break-down Spectroscopy's since they were first reported by Tarascon et al. [5,6]. Among them, undoped copper oxide (CuO) has attracted much interest owing to their high theoretical capacity, highly-stable, non-toxic, economical approach, and facile synthesis. It is a p-type semiconductor material with a band-gap energy [7-9], which is studied for various

* Correspondence: mmrahman@kau.edu.sa
[1]Center of Excellence for Advanced Materials Research (CEAMR), King Abdulaziz University, P.O. Box 80203, Jeddah 21589, KSA
[2]Chemistry Department, Faculty of Science, King Abdulaziz University, P.O. Box 80203, Jeddah 21589, KSA

applications in bio-materials [10], photo-conductive [11] electro-magnetic [12], and super-conductors mico-devices [13] etc. Various efforts have been focused toward the fabrication of nano-structured CuO to improve their performance in currently existing applications, which is considered as one of the promising artificial mediators owing to their properties and functionalities [14-21]. However, it is still a big challenge to attain high-rate capability and crystallinity of copper oxide doped semiconductor nanomaterials. It is well accepted that a smaller size of CuO can lead to higher capacity and higher surface capability. This reduces the over potential and allows faster reaction kinetics to detect the metal ions [22-24]. Therefore, the synthesis of low-dimensional CuO nanostructures is a promising approach to make a significant improvement of large-surface area and high-aspect-ratio in doped nanostructures. Due to the significant properties of semiconductors, the doped nanomaterials were attained a considerable attention in terms of controlled growth of crystalline materials in huge quantity. Various growth mechanism have been employed, including the vapor–liquid–solid growth [25], thin-film growth [26], vapor-solid growth [27], wet-chemical methods [28], and electro-spinning [29] etc. Titanium dioxide is the promising host-material as semiconductor having high photo-chemical stability and large-surface area with low economical-cost. Well-dispersed undoped titania dioxide nanostructure materials with very fine sizes are promising in many significant applications such as pigments, adsorbents and catalytic supports [30-32]. In almost all of these cases, when the dimension of nanomaterials is reduced significantly, especially to several nano-meter scales, some novel optical, morphological, and structural properties are expected, owing to the large surface-to-volume ratio [33]. In addition, the development of simple, rapid and efficient techniques has achieved a huge interest for monitoring metal ions in the environment. Several analytical methods have been applied to analyze metal ions in aqueous solutions, such as atomic absorption spectrometry [34], inductively coupled plasma-optical emission spectrometry (ICP-OES) [35], anodic stripping voltammetry [36], and ion chromatography [37]. However, analytical methods can not directly measures the metal ions, in particular at ultra-trace concentration, in aqueous systems due to the lack of sensitivity and selectivity of these methods. Therefore, an efficient separation procedure is urgently required prior to the determination of noble metals for sensitive, accurate and interference-free determination of noble metals [38].

Several analytical methods are introduced for separation of analytes including liquid-liquid extraction [39], ion-exchange [40], co-precipitation [41], cloud-point extraction [42] and solid-phase extraction (SPE) [43]. SPE is considered to be one of the most powerful methods because it minimized the solvent usage and exposure, disposal costs, and extraction time for sample preparation. Several adsorbents have appeared due to the popularity of SPE for selective extraction of analytes, such as alumina [44], C18 [45], molecular imprinted polymers, cellulose [46], silica-gel [47,48], activated carbon [49,50] and carbon nanotubes [51,52]. This study was also planned to perform the analytical efficiency of CuO-TiO$_2$ NSs phase as adsorbent on the selectivity and adsorption capacity of Fe(III) prior to its determination by ICP-OES. The selectivity of CuO-TiO$_2$ NSs towards different metal ions, including Au(III), Cd(II), Co(II), Cr(III), Fe(III), Pd(II), and Zn(II), was performed in order to study the effectiveness of CuO- TiO$_2$ NSs on the adsorption of selected metal ions. Here the calcined CuO-TiO$_2$ NSs have significant properties such as large-surface area (surface-to-volume ratio) and static adsorption capacity. These offered high adsorbent features that enhanced the direct solid-phase adsorption towards the target metal-ions for the selective detection of Fe(III) ions. Based on the selectivity study, it was found that the selectivity of nanosheet-phase was the most towards Fe (III). The static adsorption capacity for Fe(III) was also executed in this study. Results of adsorption isotherm are confirmed that the adsorption process is mainly monolayer adsorption onto surface-phase containing a finite number of adsorption sites. Adsorption data of Fe (III) are well fit with the Langmuir-classical adsorption isotherm.

Experimental section
Materials and methods
The λ_{max} (364.7 nm) of calcined CuO-TiO$_2$ NSs was evaluated with UV/visible spectroscopy (UVO-2960, LABOMED Inc.). FT-IR spectra were measured with a spectro-photometer (Spectrum-100 FT-IR) in the mid-IR range, which was purchased from Bruker, USA. The powder X-ray diffraction (XRD) prototypes were measured with X-ray diffractometer (Rigaku X-ray diffractometer, Mini-Flex 2) equipped with Cu-K$_\alpha$1 radiation (λ = 1.5406 nm) using a generator voltage (40.0 kV) and a generator current (35.0 mA). Morphology of CuO-TiO$_2$ NSs was investigated on FE-SEM instrument (FESEM; JSM-7600F, Japan). The XPS measurements were executed on a Thermo Scientific K-Alpha KA1066 spectrometer (Germany). Monochromatic AlKα x-ray radiation sources were used as excitation sources, where beam-spot size was kept in 300.0 μm. The spectra was recorded in the fixed analyzer transmission mode, where pass energy was kept at 200 eV. The scanning of the spectra was performed at lower pressures ($<10^{-8}$ Torr). 1000.0 mgL^{-1} stock standard solution of each Au(III), Cd(II), Co(II), Cr(III), Fe(III), Pd(II), and Zn(II) were purchased from Sigma-Aldrich (Milwaukee, WI, USA). All reagents were used of analytical and spectral purity

grade. Doubly distilled de-ionized water was also used throughout the experimental studies. Analytical grade of copper chloride, titanium dioxide, and sodium hydroxide was used and purchased from Sigma-Aldrich Company. ICP-OES measurements were acquired by use of a Perkin Elmer ICP-OES model Optima 4100 DV, USA. The ICP-OES instrument was optimized daily before measurement and operated as recommended by the manufacturers. The ICP-OES spectrometer was used with following parameters: FR power (1300 kW), frequency (27.12 MHz), demountable quartz torch (Ar/Ar/Ar), plasma gas (Ar) flow (15.0 $Lmin^{-1}$), auxiliary gas (Ar) flow (0.2 $Lmin^{-1}$), nebulizer gas (Ar) flow (0.8 $Lmin^{-1}$), nebulizer pressure (2.4 bar), glass spray chamber according to Scott (Ryton), sample pump flow rate (1.5 $mLmin^{-1}$), integration time (3.0 s), replicates (3), and wavelength range of monochromator (165–460 nm). Selected metal ions were measured at wavelengths of 267.60 nm for Au(III), 228.80 nm for Cd(II), 238.90 nm for Co(II), 267.72 nm for Cr(III), 259.94 nm for Fe(III), 340.46 nm for Pd(II), and 206.20 nm for Zn(II).

Samples preparation and detection procedure

Stock solutions of Au(III), Cd(II), Co(II), Cr(III), Fe(III), Pd(II) and Zn(II) were prepared in 18.2 $M\Omega \cdot cm$ distilled deionized water and stored in the dark at 4°C. For selectivity study, standard solutions (1.0 mgL^{-1}) of each metal ion were prepared and adjusted to pH value of 5.0 with acetate buffer. Then, each standard solution was individually mixed with 25.0 mg CuO-TiO$_2$ NSs. In this study, a fixed pH value of 5.0 was chosen for all metal ions in order to avoid any precipitation of other species, in particular for Fe(III). For example, Fe(III) usually forms a precipitation of Fe(OH)$_3$ with buffer solutions at pH value greater than 5.0. For the investigation of Fe(III) static adsorption capacity, the standard solutions of 0, 5.0, 10.0, 15.0, 20.0, 25.0, 30.0, 50.0, 75.0, 125.0, and 150.0 mgL^{-1} were prepared and adjusted to the optimum pH value of 5.0 and individually mixed with 25.0 mg CuO-TiO$_2$ NSs. All mixtures were mechanically shaken for 1 hr at room temperature.

Synthesis of CuO-TiO$_2$ nanosheets by a wet-chemical process

The liquid-phase precipitation was applied to prepare CuO-TiO$_2$ NSs by a wet-chemical method from CuCl$_2$ (0.1 M, 1.7048 g, 100.0 ml) and titanium dioxide (0.1 M, 0.799 g, 100.0 ml) as the precipitating agent in basic medium (pH ~ 10.5). The starting materials are put in de-ionized water to make 0.1M solution separately in round conical flask at room conditions. After addition of reducing agent (NaOH, adjusting pH at 11.0) into the
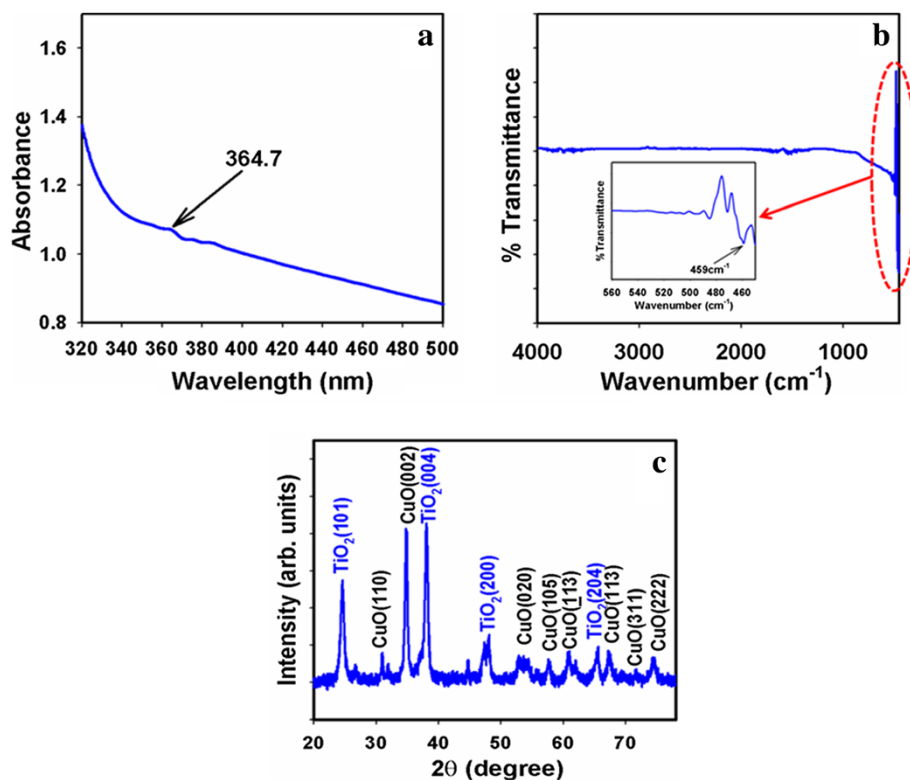

Figure 1 (a) UV/visible spectroscopy and **(b)** FT-IR spectroscopy, and **(c)** powder X-ray diffraction pattern of calcined CuO-TiO$_2$ nanosheets materials.

reactant mixtures (CuCl$_2$ & TiO$_2$), it was stirred gradually for 12 hours and placed on a hot-plate (at 150.0°C, active solution temperature ~92°C). The starting materials (CuCl$_2$, TiO$_2$, and NaOH) were used without further purification for precipitation technique. Then the solution was washed with acetone and water consecutively and kept for drying at room conditions. The as-grown powder powders were calcined at 450.0°C in muffle furnace for 5 hours. Finally, the calcined products were characterized in features of their structural, morphological, and optical properties as well as applied for the detection of metal ions uptake.

Results and discussion

Optical characterization of CuO-TiO$_2$ nanosheets

The optical property of the calcined CuO-TiO$_2$ NSs structure is one of the most important features for the evaluation of their photo-catalytic activity. The optical absorption spectra of NSs are measured by UV-visible spectrophotometer in the visible range (250.0 to 800.0 nm). In UV/visible absorption method, the outer-electrons of atoms or molecules are absorbed by incident radiation sources, which undergo electron transition from lower to higher energy levels. According to the phenomenon, the spectrum is obtained due to the optical absorption, which can be used to analyze the band-gap energy of CuO-TiO$_2$ NSs. The optical absorption measurement was carried out at ambient conditions. From the absorption spectrum, an absorbance maximum is measured using NSs at ~364.7 nm, which is presented in Figure 1a. Band-gap energy (E$_{bg}$) is calculated on the basis of the maximum absorption band of NSs and found to be 3.404 eV, according to following equation (i).

$$E_{bg} = \frac{1240}{\lambda}(eV) \tag{i}$$

Where E$_{bg}$ is the band-gap energy and λ_{max} is the wavelength (~364.7 nm) of the nanosheets. No extra peaks associated with impurities and structural defects were observed in the spectrums, which proved that the synthesized NSs control crystallinity of CuO-TiO$_2$ NSs [53].

The CuO-TiO$_2$ nanosheets were studied in term of atomic and molecular vibrations. FT-IR spectra basically in the region of 400–4000 cm^{-1} are executed at room conditions. Figure 1b displays the FT-IR spectrum of the calcined NSs structures. It represents band at 459 cm^{-1}. This observed wide vibrational band (at 459 cm^{-1}) could be assigned as a metal-oxygen (Cu-O & Ti-O) stretching vibration [54], which is demonstrated the configuration of doped nanomaterials. At low-frequency region, the vibrational bands are indicated the formation of CuO-TiO$_2$ nanosheets. To confirm the crystal phases and crystallinity of the calcined CuO-TiO$_2$ nanosheets, XRD pattern was employed and presented in Figure 1c. The obtained diffraction pattern is well matched with the base centered monoclinic CuO form. According to the
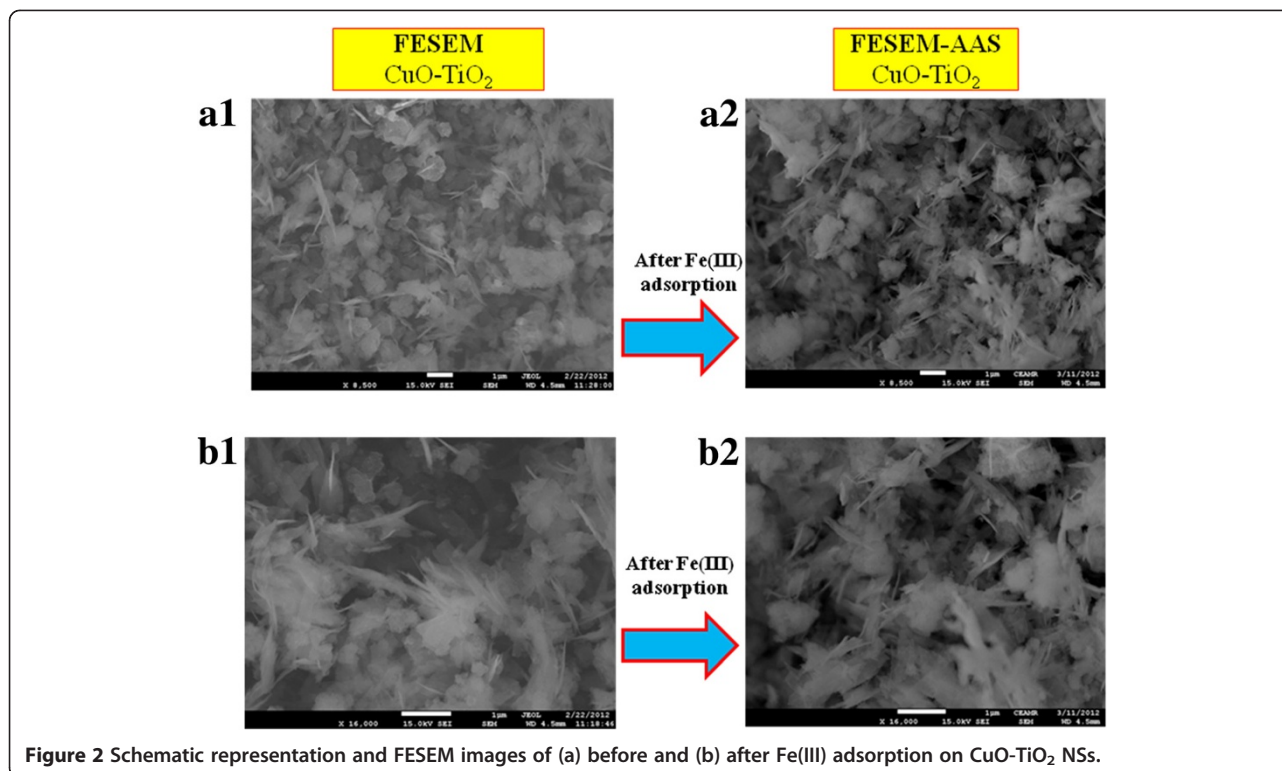

Figure 2 Schematic representation and FESEM images of (a) before and (b) after Fe(III) adsorption on CuO-TiO$_2$ NSs.
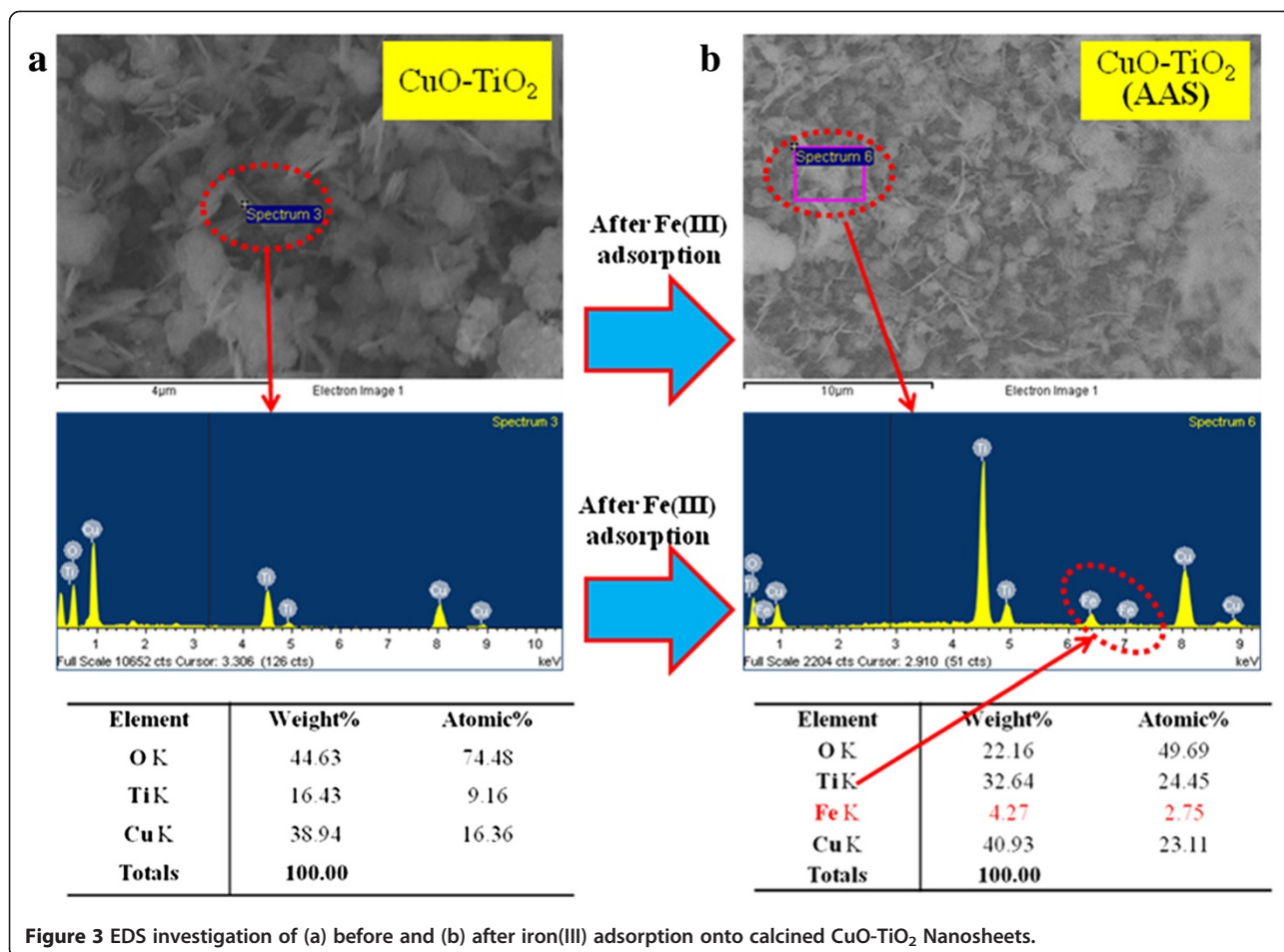
JCPDS cards (45–0937), the lattice constants for calcined CuO NSs are found to be a = 4.6853 Å, b = 3.4257 Å, and c = 5.1303 Å. The phases are found the major characteristic peaks (indicated with black-color) with indices for calcined crystalline CuO at 2θ values of (110), (002), (020), (105), ($\bar{1}$13), (113), (311), and (222), which is presented in Figure 1c. The high-intensity of diffraction peaks in the obtained pattern clearly confirmed that the doped products are well-crystalline [55]. The CuO-TiO$_2$ NSs are showed the crystalline nature of TiO$_2$ peaks lying at 2θ = 25.3° (101), 2θ = 38.1° (004), 2θ = 48.6° (200), and 2θ = 66.1(204). The preferred orientation related to the plane (004) is observed the highest magnitude. All the peaks in XRD patterns can be indexed as crystalline phases of TiO$_2$ and the diffraction data were in good agreement with JCPDS files # 021–1272 [56,57]. Crystallite size was calculated by Debye-Scherrer's formula given by equation (ii)

$$\mathbf{D} = \mathbf{K}\lambda/(\boldsymbol{\beta}\mathbf{cos}\,\theta) \qquad \text{(ii)}$$

Where D is the crystal size; λ is the wavelength of the X-ray radiation (λ = 0.15406 nm) for CuKα; K is usually taken as 0.9; and β is the line width at half-maximum height (FWHM) [58]. The average diameter and thickness of CuO-TiO$_2$ nanosheets is close to ~1.07 μm and ~21 ± 5.0 nm respectively.

High resolution FE-SEM images of calcined CuO-TiO$_2$ NSs are presented in Figure 2a to Figure 2b. Low to high-magnified FE-SEM images [Figure 2(a1) to Figure 2(b1)] of aggregated nanosheets composed microstructure materials are displayed in sheet-shape. Microstructures are composed with nano-dimensional thickness of CuO-TiO$_2$ sheets. The average length of NSs is calculated in the range of 1.0 μm to 1.3 μnm, which is close to ~1.07 ±10.0 μm. It is clearly exhibited from FE-SEM that the synthesized NS products are microstructure in regular sheet-shape with high-density of CuO-TiO$_2$. The average cross-sectional thickness of sheets is measured from the FESEM image, which is close to ~21.0 ± 5.0 nm. It is interesting to note that most of the calcined CuO-TiO$_2$ NSs are uniformly grown and possessing uniform sheet-shapes. In addition, the nano-dimensional sheets are perpendicularly arranged and aligned on the upper-portion of the calcined nanosheets. It is also proposed that the wet-chemically prepared nanostructures are composed with aggregated nanosheet composed microstructure of CuO-TiO$_2$ NSs [59].
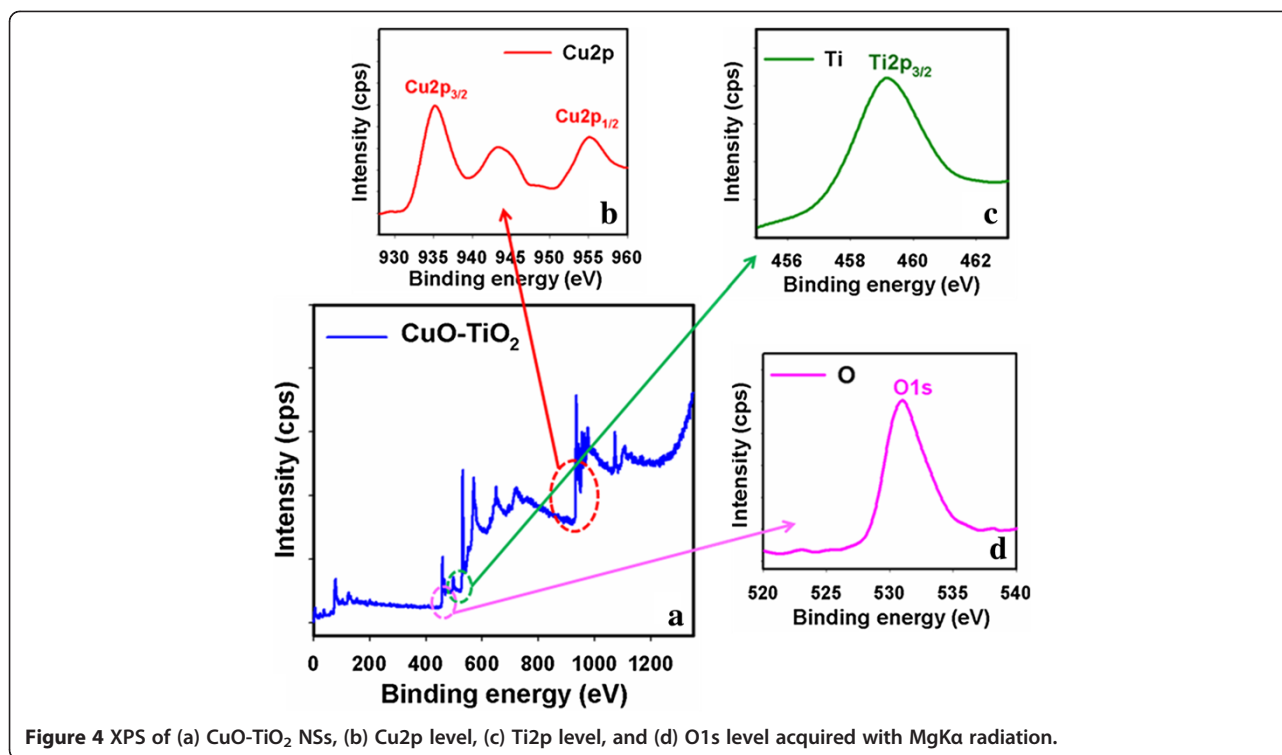

Element	Weight%	Atomic%
O K	44.63	74.48
Ti K	16.43	9.16
Cu K	38.94	16.36
Totals	100.00	

Element	Weight%	Atomic%
O K	22.16	49.69
Ti K	32.64	24.45
Fe K	4.27	2.75
Cu K	40.93	23.11
Totals	100.00	

Figure 3 EDS investigation of (a) before and (b) after iron(III) adsorption onto calcined CuO-TiO$_2$ Nanosheets.

Figure 4 XPS of (a) CuO-TiO$_2$ NSs, (b) Cu2p level, (c) Ti2p level, and (d) O1s level acquired with MgKα radiation.

The electron dispersive x-ray spectroscopy (EDS) analysis of CuO-TiO$_2$ NSs are indicated the presence of copper (Cu), titanium (Ti), and oxygen (O) composition in the pure calcined NSs before metal ions uptake [Figure 3 (a1 & b1)]. It is clearly displayed that the synthesized nanomaterial is contained only Cu, Ti, and O elements, which is presented in Figure 3(a1 & b1). No other peak related with any impurity has been detected in the FE-SEM coupled EDS, which confirms that the nanostructures are composed only with Cu (38.94%), Ti(16.43%), and O (44.63%), which is revealed in elemental analysis of Figure 3(b1) [area selected from Figure 3(a1)]. The incorporation of iron-ion onto the CuO-TiO$_2$ NSs via adsorption (i.e., physi-sorption or chemi-sorption) method is confirmed. From the EDS observation, it is demonstrated that the iron ions are adsorbed onto the NSs, which is presented in Figure 3(a2) to Figure 3(b2). The elemental composition is measured via EDS analysis of Cu(40.93%), Ti (32.64%), O(22.16%), and Fe(4.27%), which is presented as a table with the Figures 3.

X-ray photoelectron spectroscopy (XPS) is a quantitative spectroscopic method that determined the elemental-composition, kinetic energy, empirical-formula, chemical-state, binding energy, and electronic-state of the elements that present within a material. XPS spectra are acquired by irradiating a material with a beam of X-rays, while simultaneously determining the kinetic energy and number of electrons that get-away from the top one to ten nm of the material being analyzed. Here, XPS measurements were executed for CuO-TiO$_2$ nanosheets to investigate the chemical states of CuO and TiO$_2$. The XPS spectra of Cu2p and O1s are presented in Figure 4a. In Figure 4b, the spin orbit peaks of the Cu2p$_{(3/2)}$ and Cu2p$_{(1/2)}$ binding energy for all the samples appeared at around 935.2 eV and 956.1 eV respectively, which is in good agreement with the reference data for CuO [60]. In Figure 4c, the spin orbit peaks of the Ti2p$_{(3/2)}$ binding energy for codoped sample appeared around at 559.5 eV, which is in good agreement with the reference data for TiO$_2$ [61]. The O1s spectrum shows a peak at 531.9 eV in Figure 4d. The peak at 531.9 eV is assigned to lattice oxygen, may be indicated to oxygen (ie, O$_2^-$) presence in the CuO-TiO$_2$ NSs [62]. XPS compositional analyses investigated the co-existence of the two single-phase of CuO and TiO$_2$ materials. Therefore, it is concluded that the wet-chemically prepared CuO-TiO$_2$ materials have NSs phase contained two different materials. Also, this conclusion is reliable with the XRD data significantly.

Selectivity study of CuO-TiO$_2$ nanosheets

Selectivity of newly introduced CuO-TiO$_2$ NSs phase towards various metal ions was measured based on determination of the distribution coefficient of NSs phases. The distribution coefficient (K_d) can be obtained from the following equation (iii) [63]:

$$K_d = (C_o - C_e/C_e) \times (V/m) \qquad \text{(iii)}$$

Table 1 Selectivity study of CuO-TiO$_2$ NSs phase adsorption towards different metal ions at pH 5.0 and 25°C (N = 5)

Metal Ion	q_e (mgg^{-1}), TiO$_2$	q_e (mgg^{-1}), CuO-TiO$_2$	K_d (mLg^{-1}), TiO$_2$	K_d (mLg^{-1}), CuO-TiO$_2$
Fe(III)	**0.781**	**0.981**	**3557.885**	**50546.392**
Au(III)	0.150	0.153	175.938	180.638
Zn(II)	0.054	0.060	57.082	63.830
Pd(II)	0.047	0.050	49.318	52.632
Co(II)	0.036	0.040	37.344	41.667
Cd(II)	0.007	0.010	7.049	10.101
Cr(III)	0.009	0.010	9.082	10.101

where C_o and C_e refer to the initial and final concentrations before and after filtration with CuO-TiO$_2$ NSs, respectively, V is the volume (mL) and m is the weight of CuO-TiO$_2$ NSs phase (g). Distribution coefficient values of all metal ions investigated in this study are reported in Table 1. It can be clearly observed from the Table 1 that the greatest distribution coefficient value was obtained for Fe(III) with CuO-TiO$_2$ (50546.392 mLg^{-1}) as compared to pure TiO$_2$ adsorbent (3557.885 mLg^{-1}). As shown in Table 1, the amount of Fe(III) is almost extracted by CuO-TiO$_2$ phase. In addition, minimal to no change in the selectivity is observed for both CuO-TiO$_2$ and TiO$_2$ adsorbents toward other metal ions included in this study. Results of selectivity study provided that the newly synthesized CuO-TiO$_2$ phase is the most selective towards Fe(III) among all metal ions. The highest selectivity of CuO-TiO$_2$ adsorbent toward Fe(III) can be attributed to additional incorporated oxygen atoms $_{(}$donor) presented in CuO-TiO$_2$ phase, as a result of modification of TiO$_2$ with CuO. Thus, both incorporated oxygen donor atoms presented in TiO$_2$ and CuO-TiO$_2$ phases are able to selectively bind with Fe(III) through an electrostatic attraction or a chelating mechanism.
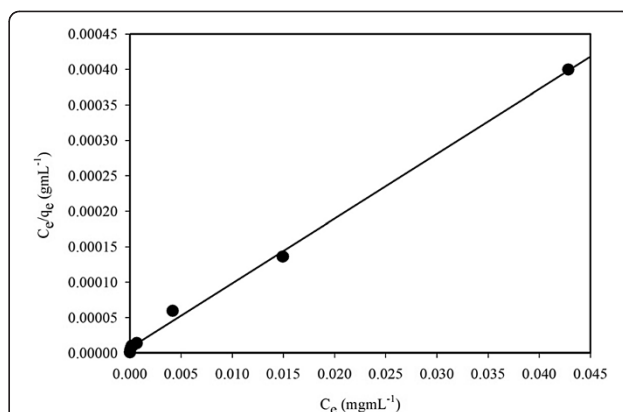
Figure 6 Langmuir adsorption isotherm model of Fe(III) adsorption on 25 mg CuO-TiO$_2$ NSs phase at pH 5.0 and 25°C. Adsorption experiments were obtained at different concentrations (0–150 mgL^{-1}) of Fe(III) under static conditions.

Static adsorption capacity

For determination of the static uptake capacity of Fe(III) on CuO-TiO$_2$ NSs phase, 25.0 mL of Fe(III) sample solutions with different concentrations (0–150.0 mgL^{-1}) were adjusted to pH 5.0 and individually mixed with 25.0 mg of CuO-TiO$_2$ NSs. These mixtures were mechanically shaken for a hr at room temperature. Static adsorption capacity was obtained using equation (iv) as follows:

$$q_e = \frac{(C_o - C_e)V}{m} \qquad \text{(iv)}$$

Where q_e represents the adsorbed Fe(III) by the CuO-TiO$_2$ NSs phase (mgg^{-1}), C_o and C_e are the initial and equilibrium concentrations of Fe(III) ion in solution (mgL^{-1}), respectively, V is the volume (L) and m is the weight of NSs phase (g). Figure 5 shows the static adsorption capacity of NSs for Fe(III) obtained from the
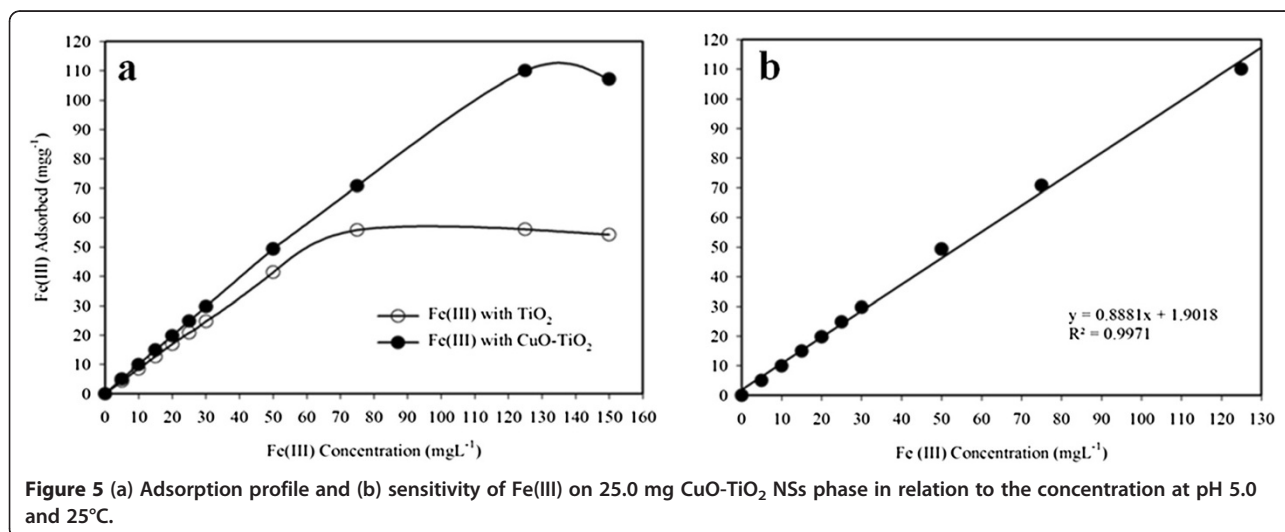
Figure 5 (a) Adsorption profile and (b) sensitivity of Fe(III) on 25.0 mg CuO-TiO$_2$ NSs phase in relation to the concentration at pH 5.0 and 25°C.

experiment of adsorption isotherm. In this study, the adsorption capacity of NSs was determined for Fe(III), which is close to be 110.06 mgg^{-1}. This is the higher adsorption capacity value obtained, which is compared with previously reports for Fe(III) in various studies such as 7.00 [64], 18.30 [65], 28.69 [66], 28.90 [67], and 173.14 [68] mgg^{-1}. Moreover, under the same batch conditions, the adsorption capacity of Fe(III) on pure TiO$_2$ and doped CuO-TiO$_2$ NSs adsorbent is estimated to be 56.06 mgg^{-1} and 110.06 mgg^{-1} respectively, which is presented in Figure 5. From this comparative study, it is concluded that the adsorption capacity for Fe(III) was improved by 96.33% with the newly synthesized CuO-TiO$_2$ NSs adsorbent as compared to pure TiO$_2$ phase. The sensitivity (slope) and linearity (R^2) of Fe(III) ion using CuO-TiO$_2$ NSs phase is calculated from the calibration plot, which is close to 0.8881 Lg^{-1} and 0.9971 respectively.

Adsorption isotherm models

Experimental equilibrium adsorption data were analyzed using different models in order to develop an equation that accurately represents the obtained results. Langmuir equation is based on an assumption of a monolayer adsorption onto a completely homogeneous surface with a finite number of identical sites and a negligible interaction between the adsorbed molecules. The Langmuir adsorption isotherm model is governed by the following relation (v) [69]:

$$C_e/q_e = (C_e/Q_o) + 1/Q_o b \qquad (v)$$

Where C_e corresponds to the equilibrium concentrations of Fe(III) ion in solution (mgmL^{-1}) and q_e is the adsorbed metal ion by the adsorbate (mgg^{-1}). The symbols Q_o and b refer to Langmuir constants related to adsorption capacity (mgg^{-1}) and energy of adsorption (Lmg^{-1}), respectively. These constants can be determined from a linear plot of C_e/q_e against C_e with a slope and intercept equal to $1/Q_o$ and $1/Q_o b$, respectively. Moreover, the essential characteristics of Langmuir-adsorption isotherm can be represented in terms of a dimension-less constant separation factor or equilibrium parameter, R_L, which is defined as $R_L = 1/(1 + bC_o)$, where b is the Langmuir constant (indicates the nature of adsorption and the shape of the isotherm); C_o the initial concentration of the analyte. The R_L value indicates the type of the isotherm, and R_L values between 0 and 1 represent a favorable adsorption [70].

The experimental isotherm data were fit-well with the Langmuir equation based on the least square fit, as shown in Figure 6, supporting the validity of Langmuir adsorption isotherm model for the adsorption process. Consequently, adsorption isotherm data was indicated that the adsorption process was mainly monolayer on a homogeneous adsorbent surface of NSs. Langmuir

constants Q_o and b are found to be 109.46 mgg^{-1} and 1.30 Lmg^{-1}, respectively. The correlation coefficient obtained from the Langmuir model is found to be $R^2 = 0.998$ for adsorption of Fe(III) on CuO-TiO$_2$ NSs. Furthermore, the static adsorption capacity (109.46 mgg^{-1}) calculated from Langmuir equation was in agreement with that (110.06 mgg^{-1}) of the experimental isotherm study. The R_L value of Fe(III) adsorption on the NSs is 0.01, indicating a highly favorable adsorption process based on the Langmuir classical adsorption isotherm model.

Conclusions

The calcined CuO-doped TiO$_2$ NSs are successfully prepared by a wet-chemical technique combined with a heat-treatment and characterized in detail in terms of their morphological, structural, and optical properties. It is displayed that the synthesized microstructures are possessed monoclinic structure having good optical properties. The static-uptake capacity of the NSs phase for selective adsorption and determination of Fe(III) in aqueous solution was investigated. Reasonable static-uptake capacity of 110.06 mgg^{-1} with NSs adsorbent for Fe(III) in aqueous solution was achieved. Adsorption data of Fe(III) was well-fit with the Langmuir adsorption isotherm model. Thus, the method may show considerable promise for using it as an effective approach for a selective separation and determination of Fe(III) in complex matrices. The obtained nanosheets composed CuO-TiO$_2$ microstructures is a promising candidate for potential application in metal ions uptake.

Authors' contributions
MMR made a significant contribution to preparation and characterization of nanomaterials, survey results, and data collection and their analysis and writing the manuscript. SBK participated in the synthesis of samples and collection of data and experimental work. HMM carried out the application part on "Metal ion uptake using doped nanomaterials" AMA has revised the manuscript for intellectual content. KAA participated in the UV/vis. and FTIR characterization of samples and collection of data and plotted the graph. All authors read and approved the final manuscript.

References
1. Morales J, Sanchez L, Martin F, Ramos-Barrado JR, Sanchez M: **Nanostructured CuO thin film electrodes prepared by spray pyrolysis: a simple method for enhancing the electrochemical performance of CuO in lithium cells.** *Electrochim Acta* 2004, **49**:4589.
2. Xiang JY, Tu JP, Zhang L, Zhou Y, Wang XL, Shi SJ: **Self-assembled synthesis of hierarchical nanostructured CuO with various morphologies and their application as anodes for lithium ion batteries.** *J Pow Sourc* 2010, **195**:313.

3. Chen L, Shet S, Tang H, Wang H, Deutsch T, Yan Y: **John Turner and Mowafak Al-Jassim. Electrochemical deposition of copper oxide nanowires for photoelectrochemical applications.** *J Mater Chem* 2010, **20**:6962–6967.

4. Grimes CA, Mor GK: **TiO₂ Nanotube Arrays: Application to Photoelectrochemical Water Splitting.** *TiO2 Nanotube Arrays* 2009, **1**:149–216.

5. Wang F, Tao W, Zhao M, Xu M, Yang S, Sun Z, Wang L, Song X: **Controlled synthesis of uniform ultrafine CuO nanowires as anode material for lithium-ion batteries.** *J Alloy Comp.* 2011, **509**:9798.

6. Poizot P, Laruelle S, Grugeon S, Dupont L, Tarascon JM: **Nano-sized transition-metal oxides as negative-electrode materials for lithium-ion batteries.** *Nature* 2000, **407**:496–499.

7. Keyson D, Volanti DP, Cavalcante LS, Simoes AZ, Varela JA, Longo E: **CuO urchin-nanostructures synthesized from a domestic hydrothermal microwave method.** *Mater Res Bull* 2008, **43**:771.

8. Drobny VF, Pulfrey DL: **Properties of reactively-sputtered copper oxide thin films.** *Thin Sol Film* 1979, **61**:89.

9. Rakhshani AE, Barakat FK: **Optical constants of reactively sputtered cupric oxide films.** *Mater Lett* 1987, **6**:37.

10. Lee SR, Rahman MM, Ishida M, Sawada K: **Fabrication of a highly sensitive penicillin sensor based on charge transfer techniques.** *Biosens Bioelectron* 2009, **24**:1877–1882.

11. Rakhshni AE: **Preparation, characteristics and photovoltaic properties of cuprous oxide-a review.** *Sol Stat Electron* 1986, **29**:7.

12. Junod A, Eckert D, Triscone G, Muller J, Reichardt W: **A study of the magnetic transitions in CuO: specific heat (1–330 K), magnetic susceptibility and phonon density of states.** *J Phys: Condens Matt* 1989, **1**:8021–8034.

13. Kosa J, Vajda I: **Environmentally friendly machining of ceramic based YBCO bulk superconductor.** *J Mater Proc Tech* 2007, **181**:48.

14. Rahman MM, Jamal A, Khan SB, Faisal M, Asiri AM: **Highly Sensitive Methanol Chemical Sensor Based on Undoped Silver Oxide Nanoparticles Prepared by a Solution Method.** *Microchim Acta* 2012, **178**:99–106.

15. Rahman MM, Jamal A, Khan SB, Faisal M, Asiri AM: **Fabrication of methanol chemical sensor based on hydrothermally prepared α-Fe₂O₃ codoped SnO₂ nanocubes.** *Talanta* 2012, **95**:18–24.

16. Pan Q, Jin H, Wang H, Yin G: **Flower-like CuO film-electrode for lithium ion batteries and the effect of surface morphology on electrochemical performance.** *Electrochim Acta* 2007, **53**:951.

17. Gao XP, Bao JL, Pan GL, Zhu HY, Huang PX, Wu F, Song DY: **Preparation and Electrochemical Performance of Polycrystalline and Single Crystalline CuO Nanorods as Anode Materials for Li Ion Battery.** *J Phys Chem B* 2004, **108**:5547.

18. Chen LB, Lu N, Xu CM, Yu HC, Wang TH: **Electrochemical performance of polycrystalline CuO nanowires as anode material for Li ion batteries.** *Electrochim Acta* 2009, **54**:4198.

19. Rahman MM, Jamal A, Khan SB, Faisal M, Asiri AM: **Fabrication of highly sensitive acetone sensor based on sonochemically prepared as-grown Ag₂O Nanostructures.** *Chem Engineer J* 2012, **192**:122–128.

20. Rahman MM, Jamal A, Khan SB, Faisal M: **Fabrication of chloroform sensors based on hydrothermally prepared low-dimensional β-Fe₂O₃ nanoparticles.** *Superlatt Microstruc* 2011, **50**:369–376.

21. Rahman MM, Jamal A, Khan SB, Faisal M: **Fabrication of highly sensitive ethanol chemical sensor based on sm-doped co₃o₄ nano-kernel by solution method.** *J Phys Chem C* 2011, **115**:9503–9510.

22. Wang HB, Pan QM, Zhao HW, Yin GP, Zuo PJ: **Fabrication of CuO film with network-like architectures through solution-immersion and their application in lithium ion batteries.** *J Pow Sourc* 2007, **167**:206.

23. Rahman MM, Khan SB, Faisal M, Asiri AM, Alamry KA: **Highly sensitive formaldehyde chemical sensor based on hydrothermally prepared spinel ZnFe₂O₄ Nanorods.** *Sens Actuator B: Chem.* 2012, **171–172**:932–937.

24. Kim MG, Cho J: **Reversible and high-capacity nanostructured electrode materials for Li-ion batteries.** *Adv Funct Mater* 2009, **19**:1497–1514.

25. Wagner RS, Ellis WC: **Vapor–liquid–solid mechanism of single crystal growth.** *App. Phys. Lett.* 1964, **4**:89.

26. Lee SR, Rahman MM, Ishida M, Sawada K: **Development of a highly-sensitive acetylcholine sensor using a charge-transfer technique on a smart biochip.** *TrAC Trend Anal Chem* 2009, **28**:196–203.

27. Jiang X, Herricks T, Xia YN: **CuO nanowires can be synthesized by heating copper substrates in air.** *Nano Lett.* 2002, **2**:1333.

28. Anandan S, Wen X, Yang S: **Room temperature growth of CuO nanorod arrays on copper and their application as a cathode in dye-sensitized solar cells.** *Mat. Chem. Phys.* 2005, **93**:35.

29. Wu H, Lin D, Pan W: **Fabrication, assembly, and electrical characterization of CuO nanofibers.** *App Phys Lett* 2006, **89**:133125.

30. Ramakrishna G, Ghosh HN: **Optical and photochemical properties of sodium dodecylbenzenesulfonate (DBS)-Capped TiO₂ nanoparticles dispersed in nonaqueous solvents.** *Langmuir* 2003, **19**:505.

31. Rahman MM, Khan SB, Faisal M, Asiri AM, Tariq MA: **Detection of aprepitant drug based on low-dimensional un-doped iron oxide nanoparticles prepared by solution method.** *Electrochim Acta* 2012, **75**:164–170.

32. Pelizzetti E, Minero C: **Mechanism of the photo-oxidative degradation of organic pollutants over TiO₂ particles.** *Elecrochim Acta* 1993, **38**:47.

33. Sahni S, Reddy SB, Murty BS: **Influence of process parameters on the synthesis of nano-titania by sol–gel route.** *Materials Science and Engineering A* 2007, **452–453**:758.

34. Mohammadi SZ, Afzali D, Pourtalebi D: **Flame atomic absorption spectrometric determination of trace amounts of lead, cadmium and nickel in different matrixes after solid phase extraction on modified multiwalled carbon nanotubes.** *Cent Eur J Chem.* 2010, **8**:662–668.

35. Cho HJ, Myung SW: **Determination of cadmium, chromium and lead in polymers by icp-oes using a high pressure asher (hpa).** *Bull. Korean Chem. Soc.* 2011, **32**:489–497.

36. Xu H, Zheng Q, Yang P, Liu J, Jin L: **Sensitive voltammetric detection of trace heavy metals in real water using multi-wall carbon nanotubes/nafion composite film electrode.** *Chin J Chem* 2011, **29**:805–812.

37. Tanikkul S, Jakmunee J, Lapanantnoppakhun S, Rayanakorn M, Sooksamiti P, Synovec RE, Christian GD, Grudpan K: **Flow injection invalve mini-column pretreatment combined with ion chromatography for cadmium, lead and zinc determination.** *Talanta* 2004, **64**:1241–1246.

38. Pyrzynska K: **Recent developments in the determination of gold by atomic spectrometry techniques.** *Spectrochim Acta Part B* 2005, **60**:1316–1322.

39. Nasu A, Yamaguchi S, Sekine T: **Solvent extraction of copper(i) and (ii) as thiocyanate complexes with tetrabutylammonium ions into chloroform and with trioctylphosphine oxide in hexane.** *Anal Sci* 1997, **13**:903–911.

40. Tao GH, Fang Z: **Dual stage preconcentration system for flame atomic absorption spectrometry using flow injection on-line ion-exchange followed by solvent extraction.** *J Anal Chem* 1998, **360**:156–160.

41. Soylak M, Erdogan ND: **Copper(ii)-rubeanic acid coprecipitation system for separation-preconcentration of trace metal ions in environmental samples for their flame atomic absorption spectrometric determinations.** *J Hazard Mater* 2006, **137**:1035–1041.

42. Manzoori JL, Abdolmohammad-Zadeh H, Amjadi M: **Simplified cloud point extraction for the preconcentration of ultra-trace amounts of gold prior to determination by electrothermal atomic absorption spectrometry.** *Microchim. Acta* 2007, **159**:71–78.

43. Fang G, Chen J, Wang J, He J, Wang S: **N-methylimidazolium ionic liquid-functionalized silica as a sorbent for selective solid-phase extraction of 12 sulfonylurea herbicides in environmental water and soil samples.** *J Chromatogr A* 2010, **1217**:1567–1574.

44. Ahmad R, Kumar R: **Adsorption of amaranth dye onto alumina reinforced polystyrene.** *Clean: Soil Air Water* 2011, **39**:74–82.

45. Pei S, Fang Z: **Flame atomic absorption spectrometric determination of silver in geological materials using a flow-injection system with on-line preconcentration by coprecipitation with diethyldithio-carbamate.** *Anal Chim Acta* 1994, **294**:185–193.

46. Rocha-de CG, Luiz-de AI, Dos-Santos RP: **Synthesis, characterization and determination of the metal ions adsorption capacity of cellulose modified with p-aminobenzoic groups.** *J Mater Res* 2004, **7**:329–334.

47. Wei K, Shu L, Guo W, Wu Y, Zeng X: **Synthesis of amino-functionalized hexagonal mesoporous silica for adsorption of pb²⁺.** *Chin J Chem* 2011, **29**:143–146.

48. Liu Y, Guo L, Zhu L, Sun X, Chen J: **Removal of cr(iii, vi) by quaternary ammonium and quaternary phosphonium ionic liquids functionalized silica materials.** *Chem Eng J* 2010, **158**:108–114.

49. Marwani HM, Albishri HM, Jalal TA, Soliman EM: **Activated carbon immobilized dithizone phase for selective adsorption and determination of Gold(iii).** *Desalin Wat Treat* 2012, **45**:128–135.

50. Marwani HM, Albishri HM, Soliman EM, Jalal TA: **Selective adsorption and determination of hexavalent chromium in water samples by chemically**

modified activated carbon with tris(hydroxymethyl)aminomethane.
J Disper Sci Technol 2012, **33**:549–555.

51. Tong S, Zhao S, Zhou W, Li R, Jia Q: **Modification of multi-walled carbon nanotubes with tannic acid for the adsorption of la, tb and lu ions.** *Microchim Acta* 2011, **174**:257–264.

52. Biparva P, Hadjmohammadi MR: **Selective separation/preconcentration of silver ion in water by multiwalled carbon nanotubes microcolumn as a sorbent.** *Clean Soil Air Wat* 2011, **39**:1081–1086.

53. Rahman MM, Jamal A, Khan SB, Faisal M: **CuO Codoped ZnO based nanostructured materials for sensitive chemical sensor applications.** *ACS Appl. Mater. Inter.* 2011, **3**:1346–1351.

54. Rahman MM, Jamal A, Khan SB, Faisal M: **Highly sensitive ethanol chemical sensor based on Ni-doped SnO$_2$ nanostructure materials.** *Biosens Bioelectron* 2011, **28**:127–134.

55. Faisal M, Khan SB, Rahman MM, Jamal A, Umar A: **Ethanol chemi-sensor: Evaluation of structural, optical and sensing properties of CuO nanosheets.** *Mater Lett* 2011, **65**:1400–1403.

56. Xu J, Li L, Yan Y, Wang H, Wang X, Fu X, Li G: **Synthesis and photoluminescence of well-dispersible anatase TiO$_2$ nanoparticles.** *J Coll inter Sci* 2008, **318**:29–34.

57. Vijayalakshmi R, Rajendran V: **Synthesis and characterization of nano-TiO$_2$ via different methods.** *Arch App Sci Res* 2012, **4**(2):1183–1190.

58. Qiu S, Kalita SJ: **Synthesis, processing and characterization of nanocrystalline titanium dioxide.** *Mater Sci Engineer A* 2006, **435–436**:327–332.

59. Abaker M, Al-Sayari SA, Baskoutas S, Rahman MM, Al-Hajry A, Kim SH, Hwang SW, Umar A: **Utilization of CuO layered hexagonal disks for room--temperature aqueous ammonia sensing application.** *AIP Conf Proc* 2010, **1370**:97–102.

60. Chusuei CC, Brookshier MA, Goodman DW: **Correlation of Relative x-ray photoelectron spectroscopy shake-up intensity with CuO particle size.** *Langmuir* 1999, **15**:2806–2808.

61. Palgrave RG, Payne DJ, Egdell RG: **Nitrogen diffusion in doped TiO$_2$ (110) single crystals: a combined XPS and SIMS study.** *J Mater Chem* 2009, **19**:8418–8425.

62. Rahman MM, Khan SB, Faisal M, Rub MA, Al-Youbi AO, Asiri AM: **Electrochemical determination of olmesartan medoxomil using hydrothermally prepared nanoparticles composed SnO$_2$–Co$_3$O$_4$ nanocubes in tablet dosage forms.** *Talanta* 2012, **99**:924–931.

63. Han DM, Fang GZ, Yan XP: **Preparation and evaluation of a molecularly imprinted sol–gel material for on-line solid-phase extraction coupled with high performance liquid chromatography for the determination of trace pentachlorophenol in water samples.** *J Chromatogr A* 2005, **1100**:131–136.

64. O'Connell DW, Birkinshaw C, O'Dwyer TF: **Heavy metal adsorbents prepared from the modification of cellulose: A review.** *Bioresour Technol* 2008, **99**:6709–6724.

65. Tokalioglu S, Yilmaz V, Kartal S, Delibas A, Soykan C: **Synthesis of a novel chelating resin and its use for selective separation and preconcentration of some trace metals in water samples.** *J Hazard Mater* 2009, **169**:593–598.

66. Zang Z, Hu Z, Li Z, He Q, Chang X: **Synthesis, characterization and application of ethylenediamine-modified multiwalled carbon nanotubes for selective solid-phase extraction and preconcentration of metal ions.** *J Hazard Mater* 2009, **172**:958–963.

67. Li Z, Chang X, Zou X, Zhu X, Nie R, Hu Z, Li R: **Chemically-modified activated carbon with ethylenediamine for selective solid-phase extraction and pre-concentration of metal ions.** *Anal Chim Acta* 2009, **632**:272–277.

68. Ghimire KN, Inoue J, Inoue K, Kawakita H, Ohto K: **Adsorptive separation of metal ions onto phosphorylated orange waste.** *Sep Sci Technol* 2008, **43**:362–375.

69. Langmuir I: **The constitution and fundamental properties of solids and liquids.** *J Am Chem Soc* 1916, **38**:2221–2295.

70. Mckay G, Blair HS, Gardener JR: **Adsorption of dyes on chitin-i: Equilibrium studies.** *J. Appl Polym Sci* 1982, **27**:3043–3057.